

Part II. Mechanistic Interpretations of Voltage Effects on Boiling Heat Transfer

An analysis of surface wetting during the application of voltage to the boiling process for isopropanol and water was made using current and voltage measurements from previous work. In the normal film boiling region, surface wetting initially contributes strongly to the increased heat transfer and, at higher voltages other factors such as local mixing and bubble characteristics appear to predominate. Based on this model, it was shown that the ratio of heat transfer increases per unit applied voltage for an annulus heated internally and heated externally (4.3 to 1) corresponded to a bubble radius of 0.052 in., assuming a linear relationship between the calculated net electrostatic force and the heat transfer increase.

In previous work, Markels and Durfee (3) studied the changes in surface wetting that occurred when direct current voltage was applied across the region of vapor formation in pool boiling isopropanol. Their results are typified by Figure 1, for which the relative resistances of the alcohol film with and without boiling were used to determine relative wetted areas (A_w/A). Data for the zero voltage case were obtained with a conductive solution of ammonium perchlorate (0.13 M) in isopropanol. The curves on Figure 1 indicate that in the normal film boiling region ($\Delta T_o > 90^\circ\text{F.}$), the relative wetted area increased with increasing voltage up to approximately 70% surface wetting (1,000 v.) and then decreased to about 67% (1,500 v.). Data for higher voltages and temperature differences presented in reference 2 support the reduction in (A_w/A) with increased voltage shown on Figure 1.

Beside changes in surface wetting, increased local mixing and changes in bubble characteristics (size, shape, and wetting angle) are regarded as the most probable major causes of the observed increases in boiling heat transfer with a voltage field applied. The mechanistic interpretation discussed in this paper is based on the current and voltage measurements that were a necessary part of the electric field experiments. These current and voltage measurements can be interpreted in terms of surface wetting that aids in the visualization of the phenomena observed.

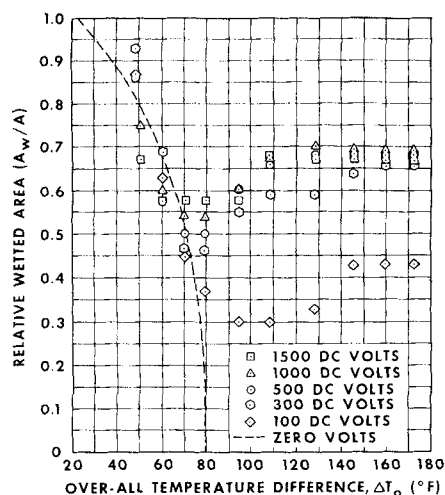


Fig. 1. Variation of relative wetted area (A_w/A) with ΔT_o at various applied d.c. voltages (pool boiling isopropanol).

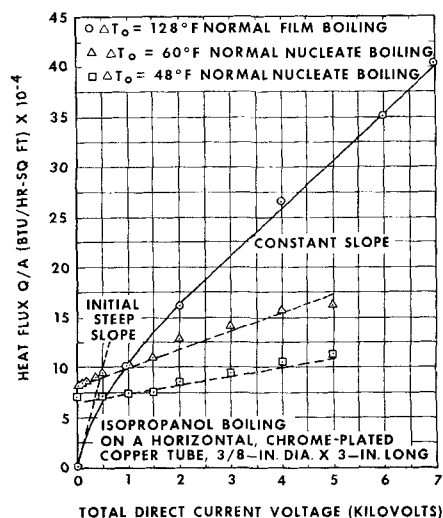


Fig. 2. Effect of d.c. voltage on heat transfer in the normal film and nucleate boiling regions for pool boiling isopropanol at one atmosphere.

ANALYSIS OF SURFACE WETTING RESULTS

In order to analyze the wetted area results it is convenient to plot Q/A vs. voltage at a particular value of ΔT_o . The solid curve in Figure 2 is typical of such plots in the normal film boiling region for both isopropanol and water. These plots show an initially steep slope of Q/A vs. voltage, which decreases to an apparently constant value as the voltage increases.

If one assumes: (1) the constant slope on the plot of Q/A vs. voltage of Figure 2 was due to increased mixing, bubble shape factors, etc. (the value of the slope is 46 B.t.u./hr.-sq. ft.-v.), and (2) the increased value of the slope over 46 in the low voltage region was due to increased surface wetting, then the difference in slope from 46 gives the contribution of surface wetting to the heat transfer increase. The contribution of surface wetting as a function of voltage for the conditions of Figure 2 is presented in Figure 3.

The slope of the curve in Figure 2 was taken as quantitatively representative of the total effect of the voltage on heat transfer. Based on the assumptions of the preceding paragraph, the deviation of the slope from a constant value of 46 represents the contribution of increased surface wetting due to the voltage, while the contribution of all other factors is constant (slope = 46). It is recognized that slopes taken from such a curve with a limited number of data points can be highly inaccurate; and, for

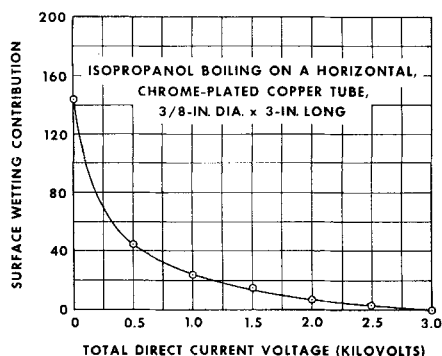


Fig. 3. Contribution of surface wetting to the rate of heat flux increase resulting from d.c. voltage application (pool boiling isopropanol at one atmosphere with $\Delta T_o = 128^\circ\text{F.}$).

this reason, the values of the slopes in Figure 3 must be considered as qualitative data only.

The above analysis is consistent with the data in Figure 1 which show: (1) the relative wetted area (A_w/A) increased with increasing voltage up to about 1,500 v. This corresponds in Figure 3 to the voltage at which the wetted area contribution begins to become negligible. (2) The rate of increase of A_w/A with voltage was steep at lower voltages and diminished as voltage was increased, in a manner similar to the curve in Figure 3.

The application of voltage to the film boiling process produces the following effects, based on visual observations and the results presented on Figure 3.

(1) The stable vapor film is subjected to an electrostatic force tending to move the liquid toward the hot surface and the vapor away from the hot surface.

(2) Perturbations in the liquid-vapor interface are accelerated toward the hot surface by the electrostatic force, thereby destabilizing the vapor film.

(3) The primary initial cause of increased heat transfer is increased wetting of the heated surface by liquid.

(4) The heat transfer rate is controlled by surface wetting until a certain amount of wetting, probably corresponding to a value of (A_w/A) near the critical packing fraction (or about 0.5), is reached.

(5) When sufficient surface wetting is reached, the process of removing heat from the region of vapor formation begins to control. At these conditions, the heat flux is increased by better mixing and more favorable bubble shape factors.

The model presented in the preceding paragraph can be tested rather simply. The model asserts that in the case where surface wetting is not important, the heat flux should be essentially proportional to voltage. These conditions apply in the normal nucleate boiling range of temperature differences. In order to demonstrate the linearity of heat flux to voltage in the normal nucleate range of ΔT_o , several representative cases from the data for pool boiling isopropanol, presented as the dashed curves in Figure 2, were chosen. These curves at constant temperature differences are linear within $\pm 10\%$, which supports the postulated physical model. The data of Bonjour et al. (1) for natural convection also support the postulated model when plotted on linear coordinates, as is shown in Figure 4.

ELECTROSTATIC FORCES APPLICABLE TO BOILING PHENOMENA

There are two types of electrostatic forces available in an electrical field that may have contributed to the observed increases in boiling heat transfer. The two forces,

one due to dielectrophoresis in a nonuniform field, and the other to the coulomb attraction between the oppositely charged plates of a condenser, would both result in displacement of a less dense fluid phase with a more dense fluid phase in a boiling situation.

Dielectrophoresis denotes motion of a dielectric liquid placed in a nonuniform electrical field, caused by induced polarization. In a two-phase situation, the phase of highest dielectric constant is accelerated toward the region of highest field strength. In the case of boiling in which the vapor is formed near the focal point of a divergent field, for example, on a heated wire, the vapor bubbles formed tend to be displaced by liquid moving toward the focal point under the influence of the dielectrophoretic force. For this simple example heat transfer would be increased by the release of more bubbles per unit time through the effect of the nonuniform field.

The principle of the condenser effect involves the force of coulomb attraction tending to draw together the oppositely charged plates of a condenser. In the case of film boiling, the solid constitutes one plate and the vapor-liquid interface serves as the other plate of a condenser. The coulomb attraction between the plates tends to accelerate the liquid toward the heat transfer surface, resulting in film destabilization, increased surface wetting, and other effects discussed in the preceding section. In the nonfilm boiling modes, the dielectric of the condenser is a zone of high bubble population. If the charge buildup on the surface of a bubble were rapid in comparison to the leakage of current through the interfaces between bubbles, coulomb attraction plus buoyancy would force bubbles away from the surface sooner than usual. This would result in smaller bubbles, higher bubble release rates, and, consequently, increased heat transfer.

Mathematical Interpretation

General expressions for the forces present from each effect are as follows:

- (1) Dielectrophoresis (or the action of a nonuniform field on a dipole within the field)

$$\bar{F} = \frac{(\epsilon - \epsilon_o)}{2} \text{ grad } (\bar{E} \cdot \bar{E}) \quad (1)$$

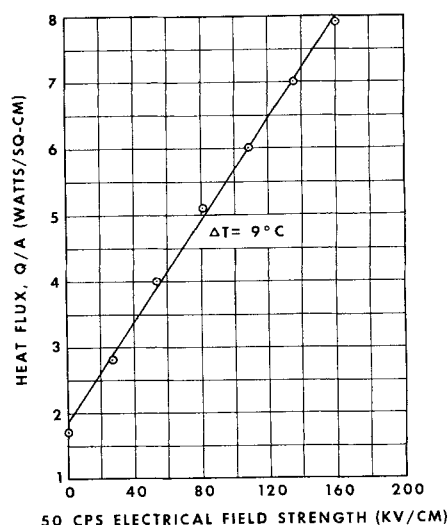


Fig. 4. Variation of heat flux with field strength for ethylether in the natural convection region, $\Delta T_s = 9^\circ\text{C.}$ (1).

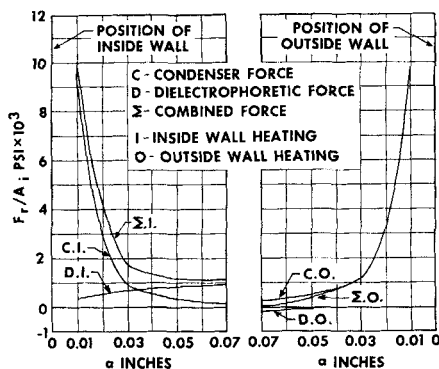


Fig. 5. Calculated force, individual and combined, for inside and outside heating as a function of bubble radius, a .

- (2) Condenser effect (resulting in a stress on the surface of a dielectric or on one plate of the condenser)

$$\bar{F}/A_i = \frac{\epsilon_o \bar{E} \cdot \bar{E}}{2} \quad (2)$$

It is readily seen from comparison of Equations (1) and (2) that the dielectrophoretic force depends on the gradient of the field strength squared, whereas the condenser effect does not. This shows that only the condenser effect would cause motion in a uniform field (where $\text{grad}(\bar{E} \cdot \bar{E}) = 0$). Equations (1) and (2) also show that polarity has no effect on the magnitude or the direction of the resulting force since the field strength vector (\bar{E}) enters into both as a squared term.

It would be more informative to compare the two effects using a specific geometry. Consider the case of two concentric cylinders of radii r_2 (outer cylinder) and r_1 (inner cylinder) with the outer cylinder charged at potential V and the inner grounded. For consistency with the interpretation of such effects on boiling, the force from dielectrophoresis will act on a bubble of radius a ($\epsilon = \epsilon_o$) immersed in a dielectric liquid ($\epsilon = \epsilon_1$; $\epsilon_1 > \epsilon_o$) at a distance $(r - r_1)$ from the inner cylinder. The dielectrophoretic force will tend to move the bubble away from the inner cylinder, and the magnitude of the force on the bubble may be used as a measure of the ability of the liquid to displace the bubble. The development of Equation (1) for the above case by Pohl (4) results in

$$F_r = 4\pi a^3 \epsilon_o K_1 \frac{K_1 - K_2}{K_2 + 2K_1} \frac{V^2}{r^3 \ln(r_1/r_2)^2} \quad (3)$$

Applying this force over the area of the bubble that is a part of a bubble layer at distance r from the center, and substituting $K_2 = 1$ gives

$$\frac{F_r}{A_i} = \frac{4\pi a^3 \epsilon_o K_1}{\pi a^2} \frac{K_1 - 1}{1 + 2K_1} \frac{V^2}{r^3 \ln(r_1/r_2)^2} \quad (4)$$

For inside heating $a = r - r_1$, giving a force on the bubble due to dielectrophoresis, which is in the direction of the desired bubble travel away from the wall of

$$\frac{F_r}{A_i} = 4(r - r_1) \epsilon_o K_1 \frac{K_1 - 1}{1 + 2K_1} \frac{V^2}{r^3 \ln(r_1/r_2)^2} \quad (5)$$

When the outside wall of the annulus (at r_2) is used as the heating surface, Equation (4), for the force per unit area due to dielectrophoresis, becomes

$$\frac{F_r}{A_i} = 4(r_2 - r) \epsilon_o K_1 \frac{K_1 - 1}{1 + 2K_1} \frac{V^2}{r^3 \ln(r_1/r_2)^2} \quad (6)$$

The dielectrophoretic force on the bubble is now in the direction of the heated wall, or opposite to the direction of desired bubble travel.

In order to compare the body force from both effects, the condenser effect will be assumed to act on a film of vapor bubbles of radius a at a distance r ($r = r_1 + a$) from the center line. This picture approximates the liquid and the vapor geometry during boiling. The force per unit area tending to accelerate the bubble away from the inner cylinder due to the condenser effect can be computed from Equation (2) as

$$\frac{F_r}{A_i} = \frac{\epsilon_o V^2}{2r^2 \ln(r_1/r)^2} \quad (7)$$

When the outside wall is heated, $r = r_2 - a$, and Equation (2) becomes

$$\frac{F_r}{A_i} = \frac{\epsilon_o V^2}{2r^2 \ln(r/r_2)^2} \quad (8)$$

In either case, the condenser effect force on the bubble is in the direction away from the heated wall, or in the direction of desired bubble travel.

Force Calculations for External and Internal Heating

Calculations were made of the dielectrophoretic and condenser forces for bubble radii of interest using Equations (5) through (8). The results are shown in Figure 5. For internal heating of the annulus the condenser force predominates for small bubbles or thin bubble films, while dielectrophoresis predominates for large bubbles. External heating of the annulus shows similar predominance of the condenser effect for small bubbles, but for large bubbles the magnitude of the two effects are roughly equal but of opposite sign. Therefore, the ratio of the electrical forces for inside vs. outside heating starts at one for the small bubbles and rises asymptotically for bubble sizes above about 0.05 in. radius as shown in Figure 6.

The calculations, made for an impressed voltage of 1,000 v., can be compared with the heat transfer results of Part I. Since the heat transfer rate is believed to be a strong function of the electrostatic forces, the ratio of the heat transfer increase per unit voltage impressed for inside to outside heating should be similar to the corresponding force ratios for the same bubble size. Data at 1,000 v. for 5.2×10^5 lb./hr.-sq. ft. at values of ΔT , well within the nucleate boiling region, was used to cal-

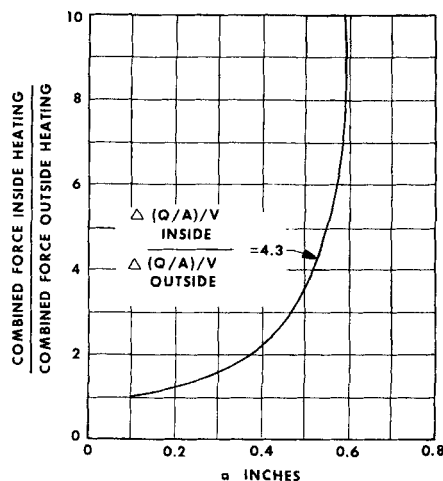


Fig. 6. Calculated force ratio for inside and outside heating as a function of bubble radius a with the measured heat flux ratio shown for comparison.

culate the heat transfer ratio. The result as shown in Figure 6 was 4.3, which corresponds to a bubble of 0.052 in., assuming the linear variation of heat flux increase with calculated force. This is a reasonable bubble size for the conditions under discussion.

ACKNOWLEDGMENT

The authors would like to acknowledge the aid of the U. S. Atomic Energy Commission (sponsors of the work) and cognizant engineer, Mr. Ronald M. Scroggins.

NOTATION

a = radius for a bubble, in.
 A = heat transfer area, sq. ft.
 A_i = area over which electrical force acts, sq. in.
 A_w = portion of heat transfer area wetted by the coolant during boiling, sq. ft.
 \bar{E} = electric field strength, v./in.
 \vec{F} = force vector, lb.
 F_r = force acting radially, lb.
 K_1 = dielectric constant, liquid
 K_2 = dielectric constant, vapor

Q = average heat transfer rate from surface, B.t.u./hr.
 r = radius $r_1 < r < r_2$, in.
 r_1 = radius of inner cylinder, in.
 r_2 = radius of outer cylinder, in.
 ΔT_o = overall temperature difference (steam temperature-water boiling point), °F.
 V = voltage impressed on boiling liquid, v.

Greek Letters

ϵ = permittivity of the dielectric medium, lb./sq. v.
 ϵ_o = permittivity of free space, lb./sq. v.

LITERATURE CITED

1. Bonjour, E., J. Verdier, and L. Weil, *Chem. Eng. Progr.*, **58**, 63-66 (1962).
2. Durfee, R. L., and M. Markels, Jr., *Summary Report* (1960-1963), USAEC, Contract No. AT(30-1)-2404 (1964).
3. Markels, M., Jr., and R. L. Durfee, *A.I.Ch.E. J.*, **10**, 63-66 (1962).
4. Pohl, H. A., *J. Appl. Phys.*, **29**, 1182-1188 (1958).

Manuscript received September 30, 1964; revision received March 9, 1965; paper accepted March 11, 1965. Paper presented at A.I.Ch.E. Boston meeting.

Model Simulation of Stirred Tank Reactors

F. S. MANNING, DAVID WOLF, and D. L. KEAIRNS

Carnegie Institute of Technology, Pittsburgh, Pennsylvania

Stirred tank reactor yields are successfully described by the following model. The impeller is considered to act as a local micro-mixer that perfectly mixes the recirculating stream down to the molecular level. All other portions of the vessel act as a large volume macro-mixer, throughout which the impeller discharge stream remains completely segregated. Changes in overall conversion due to variations in mean residence time, impeller size, and rev./min. as predicted by this micro- and macro-mixer model agree with Worrell's data for a relatively slow, second-order, irreversible reaction.

Accurate prediction of reactor yield, selectivity, and product purity is, of course, the ultimate goal of the design engineer. Any successful description of a continuous flow, stirred tank reactor must be based on close physical reality. Unfortunately, a complete theoretical analysis requires the simultaneous solution of the nonlinear, three-dimensional, partial differential equations of nonsteady state, turbulent, multicomponent mass, heat, and momentum transport; hence it is prohibitively difficult. Stirred tank reactor behavior is, therefore, often described with the help of models of varying degrees of physical reality and mathematical complexity.

PREVIOUS MODELS

The earliest and simplest isothermal, continuous flow stirred tank reactor model assumes perfect mixing or micro-mixing (5), that is, the impeller mixes the fluid down to the molecular level. No concentration gradients or fluctuations exist within the tank, hence overall yields may be computed readily from the material balance. At steady state conditions

$$\text{Input} - \text{Output} = \text{Amount reacted} \\ F c_F - F c_o = V r \quad (1)$$

For a second-order reaction of type $2A \rightarrow \text{products}$, $r = k c_o^2$ and Equation (1) yields

$$\frac{c_{\text{micro}}}{c_F} = \frac{-1 + \sqrt{1 + 4 c_F k \tau}}{2 c_F k \tau} \quad (2)$$

The outlet concentration c_o is called c_{micro} to emphasize that tank contents are completely mixed on the molecular level. In spite of the obvious oversimplification of this model, it has proved surprisingly successful in predicting overall tank yields, especially for relatively slow reactions, low fluid viscosity, and high rev./min. However, recent data (4, 14) indicate that this model fails at low rev./min.

In 1958 Danckwerts (2) suggested a macro-mix model. Now individual fluid molecules are pictured as remaining grouped together in small aggregates or lumps. These segregated lumps are assumed to be very small compared to vessel dimensions, but they are also assumed to contain a large number of molecules, for example, about 10^{12} . Reaction now occurs separately within each lump; that is, each aggregate behaves as a small, perfectly mixed, batch reactor. If the age of every lump in the exit stream is known, or, alternatively, if the residence time distribution of fluid in the vessel may be computed, then the overall vessel yield may be calculated. Stimulus-response investi-

David Wolf is at McGill University, Montreal, Canada.